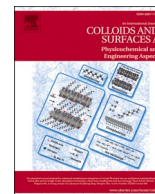




Contents lists available at ScienceDirect

Colloids and Surfaces A: Physicochemical and Engineering Aspects

journal homepage: www.elsevier.com/locate/colsurfa

Reinforcement of GO composites using rigid and flexible crosslinkers

Purneema Kaur^a, Leon Bowen^b, Lian R. Hutchings^a, Mujeeb U. Chaudhry^c, Thomas Pugh^d, Richard L. Thompson^{a,*}

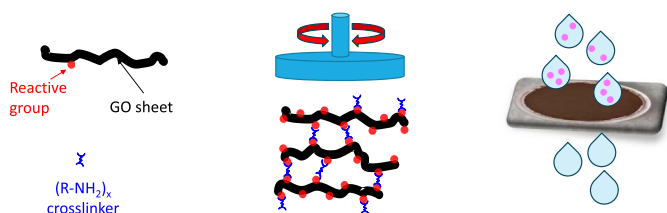
^a Department of Chemistry, Durham University, Lower Mounjoy Site, Durham DH1 3LE, United Kingdom

^b Department of Physics, Durham University, Lower Mounjoy Site, Durham DH1 3LE, United Kingdom

^c Department of Engineering, Durham University, Lower Mounjoy Site, Durham DH1 3LE, United Kingdom

^d University of Liverpool, Foundation Building, Brownlow Hill, Liverpool L69 7ZX, United Kingdom

GRAPHICAL ABSTRACT



One-pot cross-linker method for reinforcement and resilience of GO membrane coatings

ARTICLE INFO

Keywords:
Grapheneoxide
Rheology
Reinforcement
Nanocomposite
Cross-linker

ABSTRACT

Crosslinkers are important for graphene oxide (GO) plates in filtration applications because they help to define and maintain the integrity of the nanoscale structure. GO platelets were dispersed in aqueous solution and crosslinked using a simple “one-pot” process in which multi-amine functional molecules could react with carboxylic acid or epoxy groups of the GO surfaces. Strain-sweep oscillatory rheology enabled a detailed analysis of the reinforcing behaviour of crosslinkers on GO. Flow stress analysis of three different types of reinforced GO composites shows significant increases in the elastic modulus of the GO composites, compared to non-crosslinked GO. Crosslinkers were octaammonium polyhedral oligomeric silsesquioxane, (OA-POSS), a rigid cage, low M_w (0.8 kg/mol) or high M_w (25 kg/mol) chain branched polyethyleneimine, PEI (flexible). Crosslinking with either of the PEI polymers increases the yield stress of GO composites up to 20 times more than the rigid OA-POSS crosslinker, and nearly 170 times more than the non-crosslinked GO. The ‘one pot’ synthetic route employed in this work shows that maximum levels of reinforcement are relatively insensitive to crosslinker concentration. The yield stress of all three types of composites increases sharply as a function of crosslinker concentration, reaching a broad plateau, before decreasing slightly. The decrease in reinforcement at high concentrations may be attributed to the saturation of available sites on GO nanosheets inhibiting crosslinking. Composites cross-linked in-situ included a significant fraction of water which was excluded under compression. Crosslinked GO samples under compression showed an increase in the elastic modulus consistent with an increase in the effective concentration of composite. GO-coated membranes showed high rejection (up to ~90 %) of Rhodamine WT, and the resilience of these membranes was visibly improved with very low crosslinker loadings, 0.2 % w/w with respect to the mass of GO.

* Corresponding author.

E-mail address: r.l.thompson@durham.ac.uk (R.L. Thompson).

<https://doi.org/10.1016/j.colsurfa.2025.136156>

Received 19 September 2024; Received in revised form 28 November 2024; Accepted 7 January 2025

Available online 11 January 2025

0927-7757/© 2025 The Authors. Published by Elsevier B.V. This is an open access article under the CC BY license (<http://creativecommons.org/licenses/by/4.0/>).

1. Introduction

Graphene oxide has been proposed for numerous applications, including conductive transparent coatings [1], electronics [2], solar cells [3], photocatalysts [4], drilling fluids [5] and membranes [6]. Unlike graphene, GO has a substantial degree of sp^3 hybridisation, arising from the additional oxygen groups, and as a consequence, GO sheets are less flat and pack less densely than graphene. The presence of these (hydroxyl, epoxide and carboxylic acid) groups imparts the GO its hydrophilic and anti-fouling properties. The chemistry of these groups can be exploited to synthesise GO composites with tunable physical, chemical and mechanical, properties [7–10].

In lab-scale tests, GO has proven to be an excellent candidate for nanofiltration applications [11–13]. However, the industrial-scale application in this field has not yet been realised. Although, layers of GO stacked on top of each other can potentially result in laminar spacing ideal for nanofiltration applications, controlling the interlayer spacing of these sheets, especially in water, remains a challenge. This is because the hydrophilic hydroxyl and carboxylic acid groups on the GO interact favourably with water, resulting in an increase in the interlayer spacing and lower membrane rejection [14]. While the performance indicated for GO membranes appears very encouraging, it is now recognised that the stability of these membranes is the key limitation to their use. Wang et al. highlighted the problems associated with GO membranes disintegrating under water, noting that problem has significant complexities. For example, GO membranes are destabilised by low pH or monovalent cations, but stabilised by the presence of multi-valent cations [15].

GO can also experience membrane compaction under pressures used to filter water on a large scale. A more compact membrane leads to higher rejection, but the membrane flux is reduced, due to a narrowing of pathways for the transport of water molecules [16–18]. The addition of a crosslinker to control the separation between GO layers could help to maintain uniform interlayer spacing. Crosslinkers can be used to achieve a balance between membrane selectivity and flux [19–21]. GO flakes can vary in lateral size and functionalisation depending on the synthetic method and starting materials used to obtain GO [22–28]. Variation in the degree of oxidation/ functionalisation and the lateral flake size means it may require a series or combination of crosslinkers to deliver the appropriate plate separation for a range of GO materials. The desired filtration target species and the pore size of the polymeric base layer also play a key role in the determination of the “ideal” crosslinker. GO has been crosslinked with a variety of rigid [10,29] and flexible crosslinkers with encouraging results for filtration [8,30]. However, while the chemistry and morphology of these membranes are widely reported, and elsewhere there have been extensive rheological studies of GO in polymer composites [31], the detailed study of mechanical properties, necessary to understand the long-term structural stability in porous reinforced GO systems has received very little attention and is the focus of the work presented here.

We propose that in order to improve the mechanical durability of GO-modified filtration membranes, it is important to understand which measures of reinforcement such as modulus, yield stress and flow stress are significant, how these measures are related to each other and how they can be modified with different types of crosslinker. We further aim to understand how solution-based crosslinking processes impact on GO composite deposition and membrane performance. Here, the rheological behaviour of GO with three different types of crosslinkers: branched polyethyleneimine, PEI (“flexible”), of two molecular weights and octaammonium poly-octahedralsilsequioxane (OA-POSS) (“rigid”) have been compared. Both cross-linkers have reactive amine groups, which are well-established as being able to react with the surface oxygen (epoxy, carboxylic acid) groups of GO [32–34] Ranishenka et al. have previously demonstrated that PEI can be effective in adhering GO to glass or silicon surfaces [35], and the use of PEI in nanofiltration membranes is well established [36,37].

Shear rheology enables several measures of the reinforcement of crosslinked GO, which are relevant to filtration membrane performance. Elastic modulus at very low deformations, in shear or axial force gives a measure of the extent to which membrane materials may deform reversibly under pressure. This indicates how under conditions that do not damage a membrane, imposed pressure may cause changes in the membrane flux and rejection through compaction. Yield stress indicates the maximum stress, above which deformation is irreversible, so it is a useful measure of the possible operating range that a membrane material can withstand. The maximum strain at the point of yield stress is also an important criterion since this defines the extent to which a material deforms reversibly up to this limit. A further, important measure of the change in behaviour of these composites is the flow point or the flow stress. This defines the point at which these composites have more liquid-like than gel-like properties, which has relevance for processing of membrane coating materials.

In this work, we compare the extent to which different crosslinker types are able to reinforce GO membranes as a function of rigidity, size and crosslinker concentration. We also evaluate the appropriateness of possible measures of reinforcement that can be determined using a shear rheometer equipment and the reliability of these measurements. Finally, we explore the efficacy of some crosslinked GO-coated membranes in nanofiltration applications and the relationship between these results and the measures of reinforcement.

2. Materials and methods

2.1. Materials

GO prepared by the Hummers method was used as received in a 1 % aqueous dispersion. Characterisation by XRD and thermal analysis indicates an oxygen content of approximately 24 % (w/w) and interlayer separation of 0.82 nm (Supporting information S.I.1). Branched polyethyleneimines, “0.8k PEI” (Merck 408719, $M_w = 0.8$ kg/mol, $M_n = 0.6$ kg/mol) and branched “25k PEI” (Merck 408727, $M_w = 25$ kg/mol, $M_n = 10$ kg/mol) polymers were purchased from Merck KGaA. OA-POSS was purchased from Hybrid Plastics Inc. and NaOH (>99 %) from Fischer Scientific. All materials were used as received and their molecular structures are shown in Fig. 1. FTIR spectra of the materials and their mixtures are provided in supporting information (S.I.2).

2.2. Methods

2.2.1. Preparation of GO crosslinked with PEI

A series of solutions of each molecular weight (800 g mol⁻¹, $25,000$ g mol⁻¹) PEI were prepared with concentrations ranging from 2.1 mg ml⁻¹ to 21.0 mg ml⁻¹. Following a method similar to that of Guo et al., [38] 1.0 ml of each solution was added to 5.0 ml of 10 mg ml⁻¹ GO dispersion in water and shaken vigorously for 20 s, yielding a sample of 8.3 mg ml⁻¹ crosslinked GO.

2.2.2. Preparation of GO crosslinked with Octa ammonium POSS

A series of OA-POSS solutions were prepared by dissolving a defined mass of OA-POSS (between 2.1 mg to 21.0 mg) in 0.8 ml of high-purity water, followed by the addition of 0.2 ml of 0.1 M NaOH solution to make the total volume of the crosslinker solution up to 1.0 ml. This was then added to 5.0 ml of 10 mg ml⁻¹ GO dispersion in water and shaken vigorously for 20 s, yielding a sample of 8.3 mg ml⁻¹ crosslinked GO.

2.2.3. Preparation of layer-by-layer spin cast GO-crosslinker films

Films comprising two layers of GO were spin-cast onto silicon wafers for atomic force microscopy (AFM) analysis. For the non-crosslinked GO sample, 2.5 ml of 0.1 mg ml⁻¹ GO dispersion in water was dropped onto a silicon wafer while spinning at 3000 rpm and dried (layer 1). The process was repeated to add another layer of non-crosslinked GO using the same volume and concentration of GO dispersion (layer 2). For the

crosslinked GO films, 0.5 ml of 0.08 mg/ml of the crosslinker solution: 25kPEI and OA-POSS was spin-cast onto a silicon wafer, forming a base layer. Next, a layer of GO was spin-cast onto this surface using 2.5 ml of 0.1 mg/ml GO dispersion in water. These two steps were repeated in the same order to adhere a second layer of GO to the first.

2.3. Characterisation

2.3.1. Oscillatory strain tests on prepared GO-based gels

All rheological measurements were carried out using TA Instruments Discovery Hybrid (DHR-2) rotational rheometer, using a 25 mm cross-hatched plate upper geometry, and a Peltier plate was used to control the temperature to 25 °C. The initial sample equilibration (“soak”) time was 300 s, and all measurements were carried out 25 ± 0.1 °C. In strain sweep experiments, the oscillatory strain on the sample was varied from 0.01 % to 1000 %, with an angular frequency of 6.28 rad. s^{-1} , measuring 10 logarithmically spaced increments per decade of strain. The strain-dependent values of the elastic (G') and the loss (G'') moduli were measured. Measurements were repeated six times on fresh samples to establish the uncertainty in the recorded values that could arise from sample variability or sample loading. Raw data showing reproducibility between measurements are available in [supporting information](#) (S.I. 3–6).

2.3.2. Low strain elastic shear modulus, G'

The elastic shear modulus was measured in the linear region at low strain, γ , where both G' and G'' were essentially independent of strain. Data were averaged over the region $0.01 < \gamma / \% < 0.2$. The region of interest is annotated for typical data in [Fig. 2](#).

2.3.3. Yield Stress Analysis

Two different measures of yielding behaviour were considered to characterise the strain-dependent stress response of the crosslinked GO-based gels during strain-sweep experiments, [Fig. 2](#). The first method was

the G'/G'' crossover flow stress, based on stress at the intersection of the storage, G' and loss modulus, G'' of the sample were used to calculate the value of the flow stress using [Eq. 1](#),

$$\sigma_y = G' \gamma_y \quad (1)$$

where σ_y = stress at the crossover (flow) point, G' is the storage modulus and γ_y is the strain at the crossover (flow) point where G' and G'' intersect. Physically, this corresponds to the minimum stress at which the response of the material is predominantly dissipative and therefore irreversible. The second measure was the maximum oscillation yield stress, defined

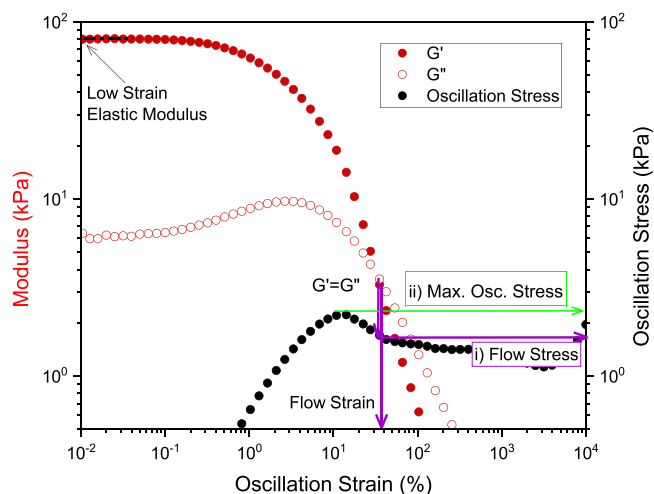


Fig. 2. Typical strain-sweep data for GO crosslinked with 25k PEI, showing the change in oscillation stress, storage and loss moduli, with the increase in oscillation strain. Annotations show two measures of yielding behaviour: flow stress (i) and maximum oscillatory stress (ii).

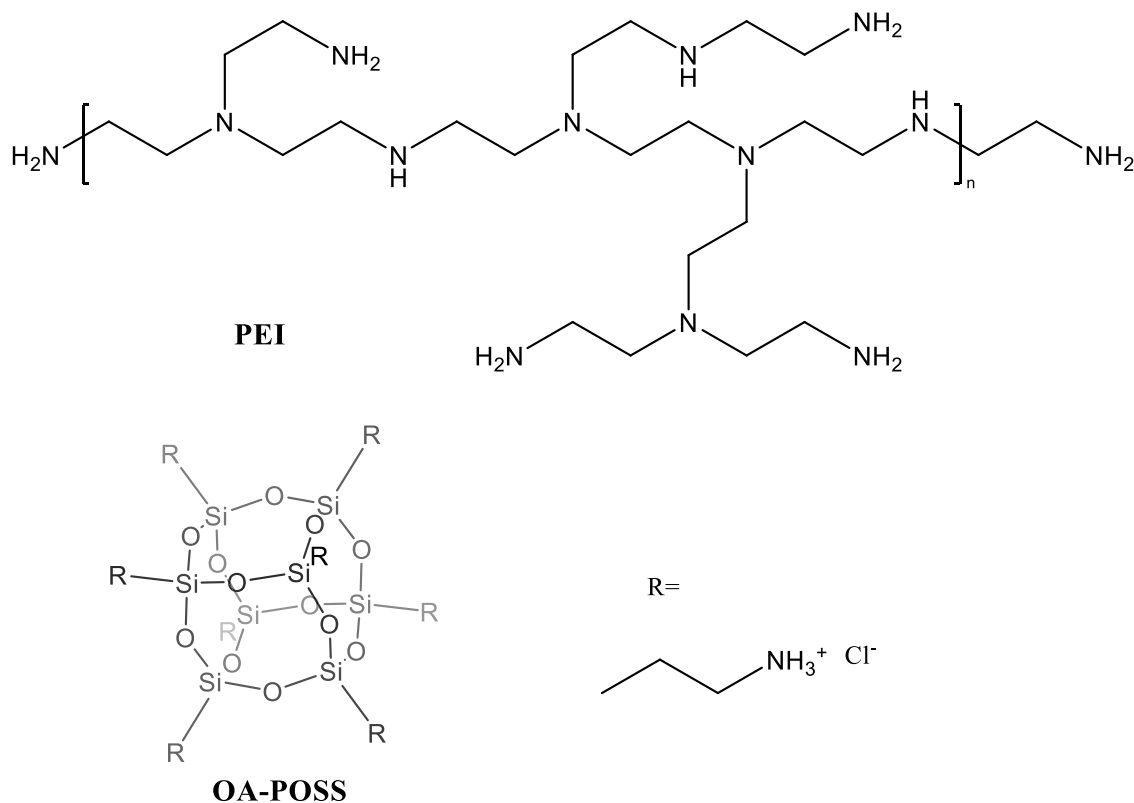


Fig. 1. Structures of crosslinkers, branched PEI (top) and OA-POSS (bottom).

as the peak value of the oscillation stress as a function of oscillation strain, Fig. 2.

2.3.4. Effect of compression on composites

When composite samples were loaded into the rheometer, the act of closing the gap between the measurement geometry and the Peltier plate was sometimes seen to cause separation between a GO-rich material under the plate and GO-sparse liquid driven out under compression. While every effort was made to minimise this phenomenon, the effect of excluding water on the crosslinked composites under compression was separately assessed to determine the impact of this behaviour on shear rheology results. Strain sweeps were measured over a small range of strain, 0.01–0.2 %, to ensure the strain applied was within the elastic region for the composite, with an angular frequency of 6.28 rad.s^{-1} , measuring 10 steps per decade. The corresponding values of G' , G'' and axial force were measured.

The distance between the geometry head and the Peltier plate was decreased after consecutive runs. The initial distance was $1300 \mu\text{m}$, which was decreased down to $500 \mu\text{m}$ with steps of $100 \mu\text{m}$ between each run. All composites tested under compression had a crosslinker: GO mass ratio (mass of crosslinker/mass of GO) of 0.17. The pressure imposed in these measurements was determined from the axial force and the surface area of the measurement geometry.

2.3.5. Atomic force microscopy

The coverage of smooth silicon substrates by GO platelets was measured by AFM. Spin-cast GO and GO/crosslinker films were analysed using the PeakForce quantitative nanomechanical mapping mode (QNM) on a Bruker Multimode 8 scanning probe microscope. $15 \mu\text{m} \times 15 \mu\text{m}$ areas of GO films, which had been spin-cast onto a clean silicon wafer were scanned, capturing images with 512 points per line. NuNanoScout 70 R probes with a spring constant of 2 N m^{-1} and a resonant frequency of 70 kHz were used. Height maps were flattened (2nd order) using Nanoscope v 1.5 software to remove the natural curvature caused by the movement of the sample relative to the cantilever.

2.3.6. Nanofiltration testing

Flux and rejection testing were carried out using a Sterlitech HP4750 dead-end cell and 47 mm diameter, 30 nm pore size polyethersulfone (PES) membranes, both supplied by (Stratlab Ltd, Cambs., UK). Membranes were coated with GO by filtration of a dilute GO dispersion onto the membrane surface, resulting in a coating over an active area of 13.3 cm^2 . 0.5 ml of 10 mg/ml GO was added to 40 ml deionised water and stirred at 1200 rpm for 2 min to obtain a homogenous dilute dispersion. 1 ml of aqueous crosslinker solution was added while stirring and stirred for a further 30 min, so that the crosslinker was present at a low mass fraction with respect to GO. The choice of crosslinker concentration was used to determine the overall mass fraction of crosslinker in the final coating. A defined volume of the crosslinked dispersion was made up to 10 ml with deionised water and vacuum filtered onto PES membranes. The volume of crosslinked dispersion was used to determine the mass of crosslinked GO that was deposited onto the PES.

Filtration of Rhodamine WT dye (Acros Organics, 20 % w/w solution) was carried out to assess the impact of modified GO coatings on flux and rejection of the membrane. Flux was measured from the mass of $4 \mu\text{g/l}$ Rhodamine WT solution passing through the membrane and rejection was determined via UV–vis spectrometry of the solutions. After filtration experiments, the membranes were inspected for damage to determine the impact of crosslinker on the resilience of the nanofiltration coating.

3. Results

Fig. 3 shows the effect of crosslinkers on the stability of GO dispersions. The initial dispersion (a) remains stable for several weeks and

appears quite stable to increasing pH to > 11 (b). However, the addition of crosslinker (c-d) induced rapid coagulation of the GO dispersed in water, consistent with crosslinking between the platelets. The control experiment using NaOH solution (pH > 11) showed no coagulation in the absence of any crosslinker, demonstrating that the impact of the crosslinkers on GO dispersion arises from their ability to form chemical bonds with some of the oxide functionalities on the GO, rather than the alkalinity of these additives (pH of PEI solutions was approximately 8–9).

Typical data (Fig. 2, further examples in supporting information S.I. 3–6) show that, with the exception of the unmodified GO samples, the rheological response has a clear linear region, where G' and G'' are almost independent of strain. At higher strains, G' decreases monotonically with increasing strain, while G'' increases slightly before decreasing more gradually. In all cases, a cross-over between G' and G'' was found, which was used to define the flow stress. There was often a maximum in oscillation yield stress values, somewhat beyond the end of the linear region, but at lower strain than the crossover in G' and G'' .

4. Discussion

We first consider the impact of the crosslinkers on the low strain elastic modulus (LSEM) in the linear region of the strain sweeps, Fig. 4.

All the crosslinkers had a significant reinforcing effect on the GO materials, giving rise to more than an order of magnitude increase in the shear elastic modulus. The PEI and POSS based crosslinkers are inexpensive, commercially available and offer a convenient platform to explore effects of cross-linker rigidity that could readily be extended to related structures. Interestingly, we observed that for all crosslinkers, there is a sharp rise in composite modulus at low concentrations followed by a plateau over which reinforcement appears to have little concentration dependence. Guo et al. [38] argue that the main effect of amines in PEI is to enable hydrogen bonding, however this does not exclude the possibility that some reinforcement arises from formation of covalently bonded crosslinks. The early work of Shechter et al. with model reactions shows that water can catalyse epoxy amine reactions and so it is likely that the amine-functional crosslinkers may also act by forming covalent bonds between GO platelets [39], and more recently Choi et al. have shown that similar reactions can proceed at room temperature [40]. The PEI crosslinkers are more effective than the OA-POSS, delivering greater reinforcement at lower loadings (by mass) and a greater maximum increase in modulus. Interestingly, there appears to be relatively little effect of the molecular weight of the PEI on the reinforcement behaviour, except at low concentrations, where the low molecular weight PEI performs better. While the origins of this difference are impossible to infer from these experiments in isolation, we note that Rissanou et al. have predicted that the infiltration of PEI into GO nanocomposites improves with decreasing molecular weight [37]. The slight reduction in modulus at very low OA-POSS concentrations may arise because the addition of crosslinker solution dilutes the GO dispersion. For both PEIs, it appears that at higher concentrations, the extent of reinforcement may decrease slightly with increasing crosslinker concentration.

The dependence of modulus on increasing crosslinker concentration can be rationalised as follows: The reaction of the crosslinkers with

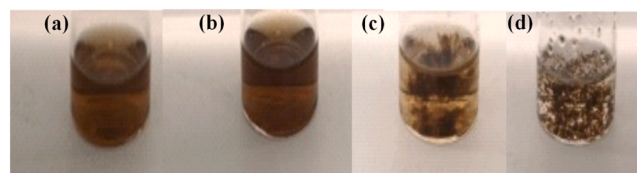


Fig. 3. (a) GO dispersion in water, (b) same GO dispersion as (a) with 1 ml 0.1 M NaOH solution added and shaken for 30 s (c) GO dispersion with 1 ml of 2 mg/ml PEI solution added showing the formation of strand-like structures, (d) same GO dispersion as (c) after shaking, showing evidence of coagulation.

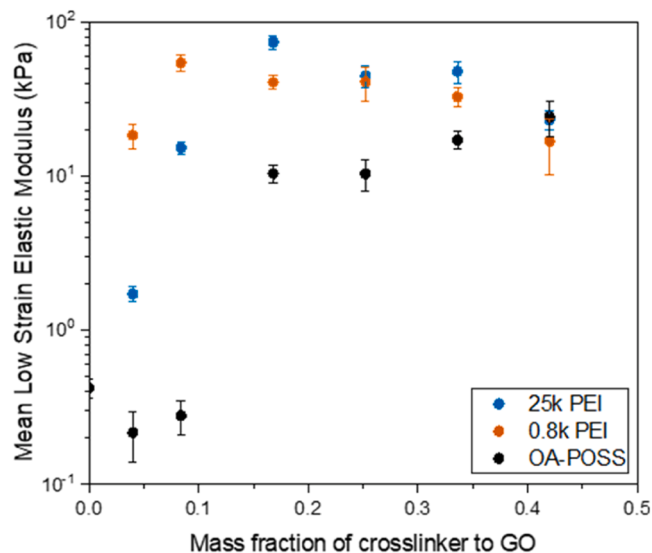


Fig. 4. The influence of crosslinker type and concentration on the mean LSEM of the 8.3 mg ml⁻¹ GO composites, based on six separate measurements for each sample.

active sites on GO, populates the surfaces of GO with functional groups that can then react and form bridges between reactive sites on other GO sheets in the dispersion. At low crosslinker loadings, the probability of crosslinking would increase with crosslinker concentration. It seems likely that the slight decrease with increasing crosslinker concentration at higher loadings could be the result of GO sheets becoming saturated, thus reducing the number of sites that are available to form crosslinks between sheets. We note that the crosslinkers may react to bond with functional groups on GO, but not to other crosslinker molecules.

For the PEIs and OA-POSS, saturation inferred from the maximum in modulus in Fig. 4 occurs at mass fractions of approximately 0.1 and 0.2 respectively. Interestingly, these values seem to correspond to very low overall coverages of GO sheets with crosslinker. Assuming complete adsorption, the mean thickness of the surface layer of crosslinker, t_{XL} can be estimated as

$$t_{XL} = \frac{1}{\rho_{XL} SSA_{GO}} \left(\frac{m_{XL}}{m_{GO}} \right) \quad (2)$$

where ρ_{XL} is the density of the crosslinker, SSA_{GO} is the specific surface area of GO and m_{XL} and m_{GO} the masses of crosslinker and GO respectively. By assuming that the GO was initially well-dispersed with SSA of order 737 m²/g [41], and that the densities of the crosslinkers are similar at ~1.27 g/cm⁻³, we estimate that the average thickness of the crosslinker layers would be of order 0.25 nm for OA-POSS and 0.12 nm for either PEI. This approximate calculation is sufficient to establish that the t_{XL} values are much smaller than the molecular dimensions of the crosslinkers (>1 nm). Therefore, it appears that the crosslinkers only partially cover the GO surfaces. From the perspective of maintaining a structure with open channels for filtration, these low fractional surface coverages would be a desirable feature.

The maximum oscillatory stress also increased with increasing concentration to a plateau, as exemplified in Fig. 5. However, the maxima at low crosslinker concentrations were often absent or ill-defined; therefore, we did not attempt to apply this measure more widely. Instead, we focus on the flow stress, defined by the crossover in G' and G'' with increasing strain, introduced in Fig. 2.

All three sets of flow stress values initially increase significantly with the addition of crosslinker (both PEIs and OA-POSS), until a maximum value is reached and then decrease slightly at the highest crosslinker concentrations, Fig. 6. This behaviour mirrors the trends already discussed for LSEM. Interestingly, this similarity between flow stress and

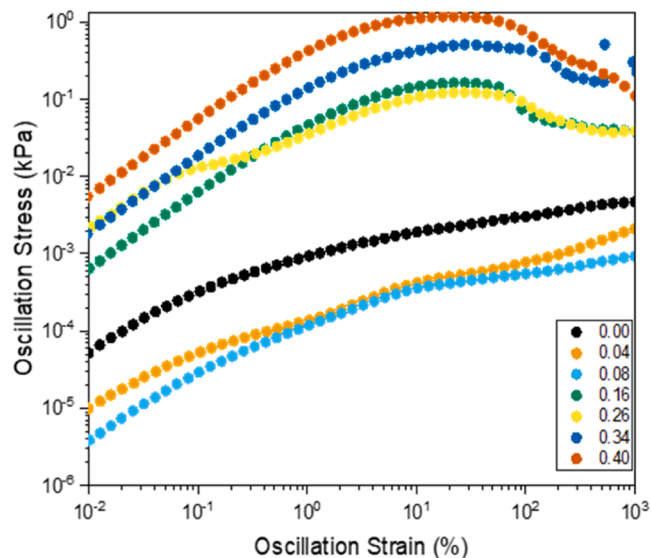


Fig. 5. Strain-dependence of oscillation stress in 8.3 mg ml⁻¹ GO/OA-POSS composite samples. The mass fraction of OA-POSS relative to GO is shown in the legend.

LSEM results suggests that there is no trade-off between the stiffness and the resilience of the composite material that might have been expected between rigid and flexible crosslinkers. Comparison of strain values at crossover (supporting information S.I. 4–6), “flow strain” showed that only modest (approximately two-fold) increases with reinforcement compared to the control GO sample without crosslinker, supporting information S.I.3. The absence of any large increase in yielding strain with crosslinking is consistent with the very high rigidity of the GO platelets; such that the stress at which crosslinkers fail is insufficient to cause significant deformation to crosslinked GO nanoplates.

As with the LSEM, the increase in flow stress with increasing crosslinker can be attributed to a more densely crosslinked GO network. Increasing the concentration of the crosslinker increases the probability that some crosslinker molecules are located where they can simultaneously bond with more than one GO platelet. The plateau in the flow stress at high concentrations is also consistent with the saturation of binding sites on the GO nanosheets, beyond which point, the probability of crosslinker molecules forming bridges between platelets may even

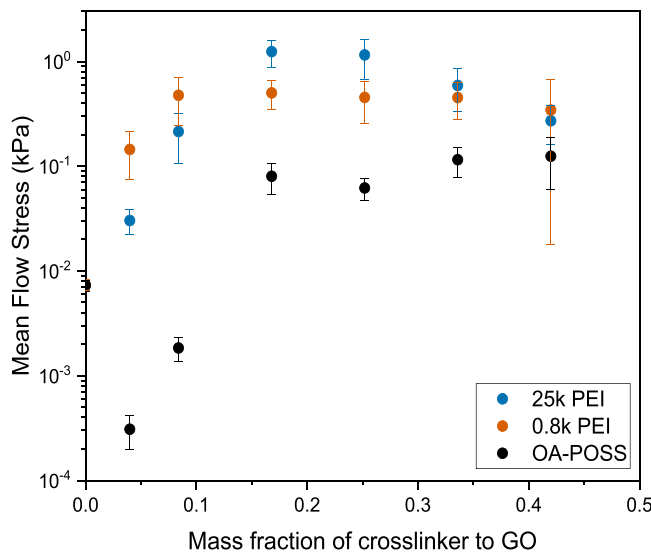


Fig. 6. The change in flow stress of different crosslinked 8.3 mg ml⁻¹ GO composites as a function of crosslinker concentration.

decrease, if all available binding sites are occupied by non-bridging crosslinker molecules.

Compared to OA-POSS, PEI shows significantly higher flow stress for either the short-chain polymer or the long-chain polymer. A maximum crossover yield stress of 1.2 kPa was achieved with the addition of 25k PEI to the GO. This is nearly 170 times higher than the yield stress of 0.007 kPa in the absence of PEI. The PEI used for this set of experiments is a branched polymer with a large proportion of primary amines available to react with the epoxy or carboxylic acid groups on the GO surface. Both PEI and POSS have multiple primary amine binding sites, but branched PEI are chains more flexible than the rigid cage structure of OA-POSS, which may result in PEI chains binding between GO sheets more readily than OA-POSS and thus forming a stronger network. Although these cross-linkers have been studied separately [8,42], we are unaware of any previous direct comparison of their cross-linking strength. The difference between these crosslinkers might be due to the flexible structure of branched PEI, as well as the synergistic interactions between PEI and GO. In the case of both PEI and OA-POSS, the amine groups can covalently bond with oxygen-containing groups on GO, but the PEI is a cationic polymer and the ionic interactions with anionic GO may give further mechanical strength to the crosslinked membranes [43]. While it is extremely challenging to determine the chemistry directly on this scale, we note that the ability of these crosslinkers to promote adhesion of GO layers onto a surface is readily illustrated by AFM, Fig. 7. These micrographs indicate that the GO dispersions contain flakes of order 1 – 10 microns size, and the thickness of single layers is ~ 1 nm, see also S.I.7. They also show that when the layer-by-layer spin-coating process used, in which solutions of cross-linker then GO were alternately spin-cast for two cycles gave rise to dramatically more GO deposition with PEI crosslinker than with OA-POSS, and somewhat more with OA-POSS, than in comparison to the control sample without crosslinker. The extent to which GO can be adhered to a silicon wafer surface follows a trend that is qualitatively consistent with the rheological measures of reinforcement: no crosslinker < OA-POSS < PEI.

At low mass fractions, the 0.8k (lower molecular weight) PEI appears to have the greatest impact on GO reinforcement, as measured by LSEM and flow stress, possibly because the larger number of smaller chains can reach a greater number of functional sites than the 25k PEI. Although comparable in mass to the 0.8k PEI, the rigid OA-POSS ($M_w \sim 1.0$ kg/mol) is consistently less effective as a reinforcing crosslinker than either PEI. The longer chain PEI confers slightly higher flow stress values to GO composites than the shorter chain PEI for PEI:GO mass fractions above 0.1, which may reflect the greater capacity of the larger PEI molecule to form bridges between adjacent GO flakes. The slightly irregular surface

of GO may prevent uniformly close contact between adjacent GO sheets and a longer crosslinker chain length may enable more interfacial bonding between the GO sheets and the crosslinker [43], resulting in a higher elastic modulus and yield stress.

Our rheological analysis (Figs. 4, 5, 6 and supporting information) shows significant variations in some of the measurements that were averaged from six repeats of each sample. This could be attributed to some variation in the effective concentration of composite in the measurement gap arising from the loading process. It was seen that when the rheometer head was brought down onto a composite sample, the excess material ‘squeezed out’ from the edges of the measurement appeared to be predominantly water. It is likely that concentration of GO in the measurement system could increase significantly with decreasing gap size and that this uncertainty from the sample loading process is the dominant source of error in the rheological characterisation. Similar behaviour is well-known for hard colloids (“self-filtration”) under compression [44]. To investigate the effect of water exclusion, low amplitude strain sweep experiments were carried out on samples in which the distance between the geometry head and sample plate was incrementally reduced.

Raw data are provided in the supporting information, S.I.8–10. Excluding water and therefore forcing the crosslinked agglomerates together results in an increase in the axial force exerted by the sample against the top plate of the rheometer for the GO composites, Fig. 8. Axial force measurements, normalised with respect to geometry area and presented as pressure, show that the PEI reinforced GO composites are more resistant to compression than the OA-POSS reinforced GO samples. We note that this straightforward test may be valuable in directly predicting the extent of compaction during filtration under high pressure. In these experiments, the more rigid cross linker molecules appear to result in a less rigid composite material. A similar trend in the dependence of the elastic shear modulus under compression for these cross linkers, S.I.11. The LSEM increases significantly when the sample gap is reduced, which is consistent with an increase in effective concentration of GO in the measurement system with decreasing gap size.

The rheological response of composites is a particularly important measure for GO coatings for porous polymer membranes because these properties are relevant for the formation of the coating and its properties when in use. The flow stress values of these samples provides a convenient measure of the point at which their behaviour transitions from elastic solid to viscous liquid [45]. For preparation of membrane coatings, some flow is necessary unless the coating can be prepared in-situ on the membrane surface; whereas during in-use filtration elastic behaviour is required for reliable performance. We believe that understanding the balance between these properties is of considerable practical value

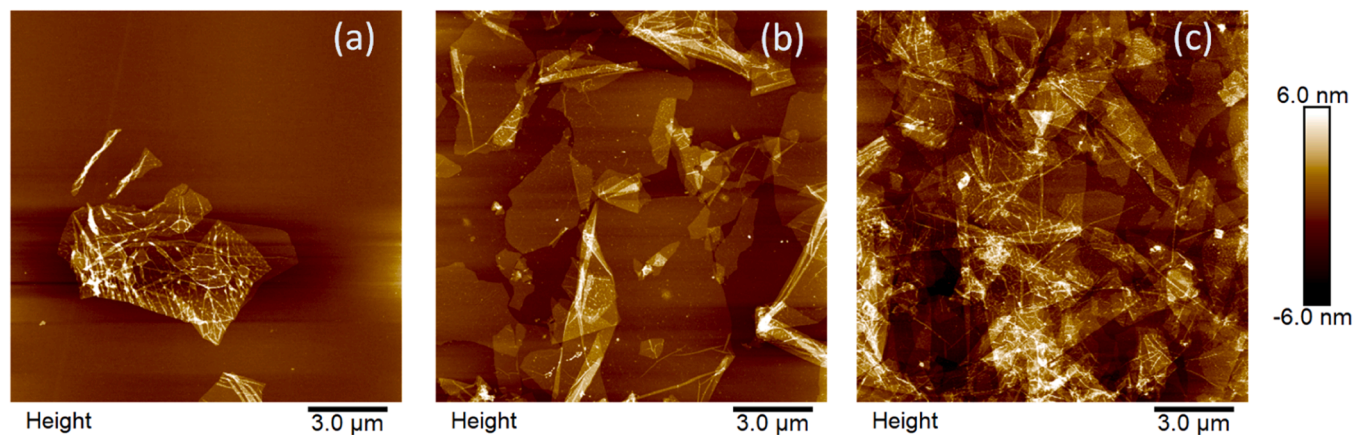


Fig. 7. Atomic force micrographs, 15 μm scans of silicon wafer surface after two cycles of spin-coating a cross-linker solution, then a GO dispersion. In all images, the vertical scale is fixed at 12 nm to highlight the impacts of a) no crosslinker between GO depositions b) OA-POSS crosslinker before each GO deposition c) 25kPEI before each GO deposition. In all three cases the same amount of GO has been used and in the case of crosslinked GO, the same amount of crosslinker has been used.

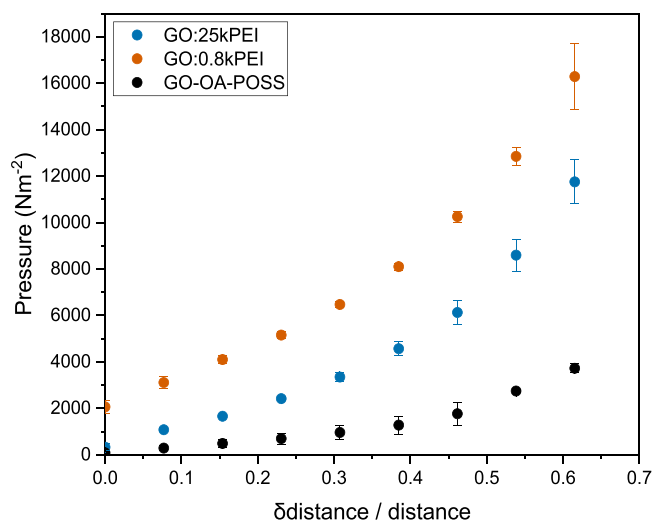


Fig. 8. Impact of compression on pressure through axial force on 0.17: 1 (w/w) crosslinker: GO composites using three different crosslinkers.

for successful preparation of effective nanofiltration coatings.

Nanofiltration of Rhodamine WT was explored for 30 nm PES membranes, which were coated with GO. AFM height maps of the coated and uncoated membrane surfaces are provided in [supporting information](#), S.I.12. In the absence of GO, the Rhodamine WT molecules ($M_w = 567$ g/mol), which are of order 1 nm, are not rejected by the bare membrane and rejection was only significant for GO-coated membranes. The cross-linker is not expected to have a large effect on the GO platelet separation but should help to minimise changes to this separation when the GO is exposed to aqueous solutions. The crosslinker loadings that gave the greatest reinforcement in our rheology experiments caused rapid coagulation of GO in solution, to such an extent that it was not possible to form consistent coatings on PES membranes. While increasing the cross-linker concentration at fixed GO concentration would be expected to yield a more robust coating, it was found that the more strongly crosslinked GO in solution did not coat well onto the membrane, and the high fluxes measured corresponded to poor rejection [supporting information](#) S.I.13. On a macroscopic scale, this variation in coverage meant not all pores on the PES membranes were covered with the crosslinked GO, and nanofiltration results were poor. For this reason, much lower mass fractions of crosslinker to GO were used for filtration studies. [Figs. 9 and 10](#) show the impact of GO coating mass deposited and crosslinker type on the membrane performance. The crosslinker, when present, was at a mass fraction of 0.2 % (w/w) with respect to GO. The decreasing flux observed with increasing GO coating thickness, [Fig. 9](#), is consistent with the more tortuous path through the membrane associated with thicker coatings. Interestingly, the correlation with rejection, [Fig. 10](#), is less clear, but a significant level of rejection was measured in most cases and rejection could be as high as 90 %. We believe, given the stochastic nature of rejection results, that low rejection levels are primarily a consequence of incomplete coverage of the PES by the GO coating. It appears that higher cross-link densities cause greater coagulation in the solution, and more dense aggregates with tortuous paths, but that there are greater opportunities for spaces to exist between aggregates. Overall, the results for rejection indicate that consistency of the membrane coating is the limiting factor for their effectiveness. The SEM micrograph included in [supporting information](#), S.I.14, indicates that even for membranes that appear to be completely covered with GO, the aggregated GO gives rise to significant variations in areal coverage. [Fig. 11](#) shows that after filtration experiments, significant degradation of the non-crosslinked GO coating is apparent, whereas the GO-coatings with 0.8k PEI crosslinker, even at very low loadings have qualitatively better resilience, and appear unaltered from

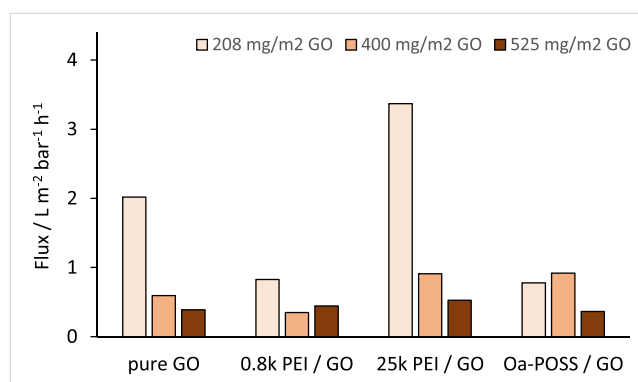


Fig. 9. Influence of GO coating thickness (mg/m² deposited) and crosslinker species on filtrate flux of Rhodamine WT solution. The crosslinker mass fraction was 0.002 with respect to GO.

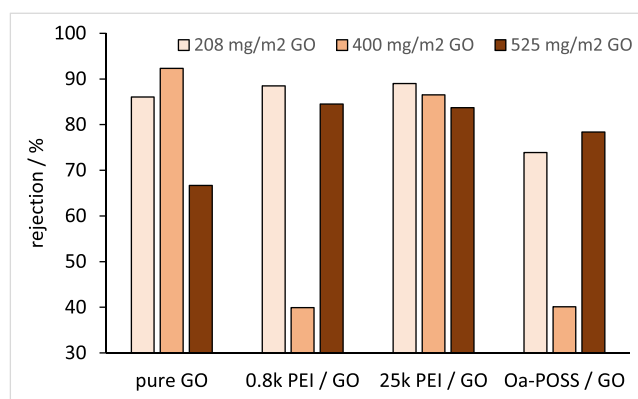


Fig. 10. Influence of GO coating thickness (mg m⁻² deposited) and crosslinker species on rejection of Rhodamine WT solution from aqueous solution in dead-end cell test. The crosslinker mass fraction was 0.002 with respect to GO.

the appearance of the original coating.

5. Conclusion

A detailed analysis of GO reinforcement using a facile crosslinking strategy shows that significant, quantifiable reinforcement of GO composites is possible at low crosslinker loadings with a simple one-pot route. Surprisingly, the flexibility of the crosslinker had almost no impact on the flexibility of the resulting reinforced composite, and there was only a modest increase in the strain at which the GO composites yielded. GO composite materials that were crosslinked with flexible PEI

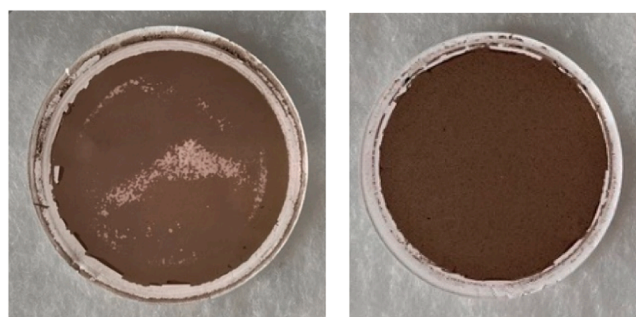


Fig. 11. Image of 208 mg m⁻² GO-coated PES membranes after filtration experiments, (left) without crosslinker and (right) with 0.002 mass fraction 0.8k PEI with respect to GO.

linkers offered greater shear modulus and greater elastic modulus under compression than their counterparts that were crosslinked with rigid OA-POSS nanoparticles. This result was attributed to the greater ability of the flexible PEI crosslinker to form bridges that span between functional groups of adjacent GO sheets. Two measures of reinforcement were identified as being most useful; the low strain elastic modulus which provides a measure of resistance to deformation under elastic conditions, and the flow stress, at which point the behaviour of the composite transitions from elastic solid to viscous liquid. Both measures of reinforcement showed qualitatively similar trends. At low crosslinker loadings there was a sharp increase in reinforcement with increasing crosslinker concentration before a broad plateau, and at the highest crosslinker concentrations explored, there was some evidence for a decrease in modulus and flow stress. The concentration dependence was consistent with the probability of forming crosslinks between adjacent GO sheets when the crosslinker was introduced to the dispersion.

The levels of crosslinker that gave the greatest reinforcement yielded a material that was difficult to coat evenly onto a PES membrane. However, even at very low PEI crosslinker loadings, membranes could be coated with reinforced GO, which improved their resilience without compromising flux or rejection with respect to Rhodamine WT.

Our work has highlighted the importance of crosslinkers not only for defining rejection or selectivity of membranes via interlayer spacing, but also for their ability to generate a membrane that can withstand the stresses imposed during filtration processes. Our results also highlight the need for engineering solutions to accompany crosslinking chemistry in order to generate truly resilient nanofiltration membranes.

CRedit authorship contribution statement

Purneema Kaur: Writing – original draft, Methodology, Investigation, Formal analysis, Data curation. **Leon Bowen:** Methodology, Data curation. **Lian R. Hutchings:** Writing – review & editing, Supervision, Methodology. **Richard L. Thompson:** Writing – review & editing, Writing – original draft, Supervision, Project administration, Methodology, Formal analysis, Conceptualization. **Mujeeb U. Chaudhry:** Writing – review & editing, Supervision, Methodology. **Thomas Pugh:** Writing – review & editing, Supervision, Project administration, Conceptualization.

Declaration of Competing Interest

The authors declare that they have no known competing financial interests or personal relationships that could have appeared to influence the work reported in this paper.

Acknowledgement

We thank EU-RDF for financial support of this work through the ERDF – Intensive Industrial Innovation Programme – 25R17P01847.

Appendix A. Supporting information

Supplementary data associated with this article can be found in the online version at [doi:10.1016/j.colsurfa.2025.136156](https://doi.org/10.1016/j.colsurfa.2025.136156).

Data availability

Data will be made available on request.

References

- [1] S. Wu, Z. Yin, Q. He, X. Huang, X. Zhou, H. Zhang, Electrochemical deposition of semiconductor oxides on reduced graphene oxide-based flexible, transparent, and conductive electrodes, *J. Phys. Chem. C* 114 (2010) 11816–11821.
- [2] M. Soni, P. Kumar, J. Pandey, S.K. Sharma, A. Soni, Scalable and site specific functionalization of reduced graphene oxide for circuit elements and flexible electronics, *Carbon* 128 (2018) 172–178.
- [3] L.A. Dobrzański, M. Prokopiuk, W. Prokopowicz, A. Drygała, A. Wierzbička, K. Lukaszewicz, M. Szindler, Carbon nanomaterials application as a counter electrode for dye-sensitized solar cells, *Arch. Metall. Mater.* 62 (2017) 27–32.
- [4] C. Yang, X. You, J. Cheng, H. Zheng, Y. Chen, A novel visible-light-driven In-based MOF/graphene oxide composite photocatalyst with enhanced photocatalytic activity toward the degradation of amoxicillin, *Appl. Catal. B: Environ.* 200 (2017) 673–680.
- [5] A.H. Abdullah, S. Ridha, D.F. Mohshim, M.A. Maoinser, An experimental investigation into the rheological behavior and filtration loss properties of water-based drilling fluid enhanced with a polyethyleneimine-grafted graphene oxide nanocomposite, *RSC Adv.* 14 (2024) 10431–10444.
- [6] F. Ma, Z. Li, H. Zhao, Y. Geng, W. Zhou, Q. Li, L. Zhang, Potential application of graphene oxide membranes for removal of Cs(I) and Sr(II) from high level-liquid waste, *Sep. Purif. Technol.* 188 (2017) 523–529.
- [7] A.M. Joseph, B. Nagendra, K.P. Surendran, E.B. Gowd, Sustainable in situ approach to covalently functionalize graphene oxide with POSS molecules possessing extremely low dielectric behavior, *Langmuir* 35 (2019) 4672–4681.
- [8] P.S. Parsamehr, M. Zahed, M.A. Tofighy, T. Mohammadi, M. Rezakazemi, Preparation of novel cross-linked graphene oxide membrane for desalination applications using (EDC and NHS)-activated graphene oxide and PEI, *Desalination* 468 (2019) 114079.
- [9] D.H. Seo, S. Pineda, Y.C. Woo, M. Xie, A.T. Murdock, E.Y.M. Ang, Y. Jiao, M. J. Park, S.I. Lim, M. Lawn, F.F. Borghi, Z.J. Han, S. Gray, G. Millar, A. Du, H. K. Shon, T.Y. Ng, K. Ostrikov, Anti-fouling graphene-based membranes for effective water desalination, *Nat. Commun.* 9 (2018) 683.
- [10] L. Yang, X. Liu, H. Wu, S. Wang, X. Liang, L. Ma, Y. Ren, Y. Wu, Y. Liu, M. Sun, Z. Jiang, Amino-functionalized POSS nanocage intercalated graphene oxide membranes for efficient biogas upgrading, *J. Membr. Sci.* 596 (2020) 117733.
- [11] A. Alabi, L. Cseri, A. Al Hajaj, G. Szekeley, P. Budd, L. Zou, Electrostatically-coupled graphene oxide nanocomposite cation exchange membrane, *J. Membr. Sci.* 594 (2020) 117457.
- [12] H.-R. Chae, J. Lee, C.-H. Lee, I.-C. Kim, P.-K. Park, Graphene oxide-embedded thin-film composite reverse osmosis membrane with high flux, anti-biofouling, and chlorine resistance, *J. Membr. Sci.* 483 (2015) 128–135.
- [13] D. Cohen-Tanugi, J.C. Grossman, Water desalination across nanoporous graphene, *Nano Lett.* 12 (2012) 3602–3608.
- [14] N. Wei, C. Lv, Z. Xu, Wetting of graphene oxide: a molecular dynamics study, *Langmuir* 30 (2014) 3572–3578.
- [15] Z. Wang, F. He, J. Guo, S. Peng, X.Q. Cheng, Y. Zhang, E. Drioli, A. Figoli, Y. Li, L. Shao, The stability of a graphene oxide (GO) nanofiltration (NF) membrane in an aqueous environment: progress and challenges, *Mater. Adv.* 1 (2020) 554–568.
- [16] J.Y. Chong, B. Wang, C. Mattevi, K. Li, Dynamic microstructure of graphene oxide membranes and the permeation flux, *J. Membr. Sci.* 549 (2018) 385–392.
- [17] K.M. Persson, V. Gekas, G. Trägårdh, Study of membrane compaction and its influence on ultrafiltration water permeability, *J. Membr. Sci.* 100 (1995) 155–162.
- [18] C.D. Wood, M.J. Palmeri, K.W. Putz, Z. An, S.T. Nguyen, L. Catherine Brinson, Hierarchical structure and properties of graphene oxide papers, *J. Appl. Mech.* 80 (2013).
- [19] F. Pan, Y. Li, Y. Song, M. Wang, Y. Zhang, H. Yang, H. Wang, Z. Jiang, Graphene oxide membranes with fixed interlayer distance via dual crosslinkers for efficient liquid molecular separations, *J. Membr. Sci.* 595 (2020) 117486.
- [20] D. Zhao, J. Zhao, Y. Ji, G. Liu, S. Liu, W. Jin, Facilitated water-selective permeation via PEGylation of graphene oxide membrane, *J. Membr. Sci.* 567 (2018) 311–320.
- [21] S. Zheng, B. Mi, Emerging investigators series: silica-crosslinked graphene oxide membrane and its unique capability in removing neutral organic molecules from water, *Environ. Sci.: Water Res. Technol.* 2 (2016) 717–725.
- [22] B.C. Brodie, XIII. On the atomic weight of graphite, *Philos. Trans. R. Soc. Lond.* 149 (1997) 249–259.
- [23] Z.-L. Chen, F.-Y. Kam, R.G.S. Goh, J. Song, G.-K. Lim, L.-L. Chua, Influence of graphite source on chemical oxidative reactivity, *Chem. Mater.* 25 (2013) 2944–2949.
- [24] C.K. Chua, Z. Sofer, M. Pumera, Graphite oxides: effects of permanganate and chlorate oxidants on the oxygen composition, *Chem. – A Eur. J.* 18 (2012) 13453–13459.
- [25] D.R. Dreyer, A.D. Todd, C.W. Bielawski, Harnessing the chemistry of graphene oxide, *Chem. Soc. Rev.* 43 (2014) 5288–5301.
- [26] U. Hofmann, E. König, Untersuchungen über Graphitoxid, *Z. F. üR. Anorg. und Allg. Chem.* 234 (1937) 311–336.
- [27] D.C. Marcano, D.V. Kosynkin, J.M. Berlin, A. Sinitskii, Z. Sun, A. Slesarev, L. B. Alemany, W. Lu, J.M. Tour, Improved synthesis of graphene oxide, *ACS Nano* 4 (2010) 4806–4814.
- [28] L. Staudenmaier, Verfahren zur Darstellung der Graphitsäure, *Ber. der Dtsch. Chem. Ges.* 31 (1898) 1481–1487.
- [29] L. Dong, M. Li, S. Zhang, X. Si, Y. Bai, C. Zhang, NH₂-Fe₃O₄-regulated graphene oxide membranes with well-defined laminar nanochannels for desalination of dye solutions, *Desalination* 476 (2020) 114227.
- [30] A. Alkhouzaam, H. Qiblawey, M. Khraisheh, Polydopamine functionalized graphene oxide as membrane nanofiller: spectral and structural studies, *Membranes* 11 (2021) 86–102.
- [31] F. Del Giudice, A.Q. Shen, Shear rheology of graphene oxide dispersions, *Curr. Opin. Chem. Eng.* 16 (2017) 23–30.

- [32] S. Park, D.A. Dikin, S.T. Nguyen, R.S. Ruoff, Graphene oxide sheets chemically cross-linked by polyallylamine, *J. Phys. Chem. C* 113 (2009) 15801–15804.
- [33] L.Q. Xu, W.J. Yang, K.-G. Neoh, E.-T. Kang, G.D. Fu, Dopamine-induced reduction and functionalization of graphene oxide nanosheets, *Macromolecules* 43 (2010) 8336–8339.
- [34] S. Chakraborty, S. Saha, V.R. Dhanak, K. Biswas, M. Barbezat, G.P. Terrasi, A. K. Chakraborty, High yield synthesis of amine functionalized graphene oxide and its surface properties, *RSC Adv.* 6 (2016) 67916–67924.
- [35] B. Ranishenka, E. Ulashchik, M. Tatulchenkov, O. Sharko, A. Panarin, N. Dremova, V. Shmanai, Graphene oxide functionalization via epoxide ring opening in bioconjugation compatible conditions, *FlatChem* 27 (2021) 100235.
- [36] Q. Nan, P. Li, B. Cao, Fabrication of positively charged nanofiltration membrane via the layer-by-layer assembly of graphene oxide and polyethylenimine for desalination, *Appl. Surf. Sci.* 387 (2016) 521–528.
- [37] A. Rissanou, A. Konstantinou, K. Karatasos, Morphology and dynamics in hydrated graphene oxide/branched poly(ethyleneimine) nanocomposites: an in silico investigation, *Nanomaterials* 13 (2023) 1865–1884.
- [38] H. Guo, T. Jiao, Q. Zhang, W. Guo, Q. Peng, X. Yan, Preparation of graphene oxide-based hydrogels as efficient dye adsorbents for wastewater treatment, *Nanoscale Res. Lett.* 10 (2015) 272.
- [39] L. Shechter, J. Wynstra, R.P. Kurkijy, Glycidyl ether reactions with amines, *Ind. Eng. Chem.* 48 (1956) 94–97.
- [40] W. Choi, K. Min, C. Kim, Y.S. Ko, J.W. Jeon, H. Seo, Y.-K. Park, M. Choi, Epoxide-functionalization of polyethyleneimine for synthesis of stable carbon dioxide adsorbent in temperature swing adsorption, *Nat. Commun.* 7 (2016) 12640.
- [41] P. Montes-Navajas, N.G. Asenjo, R. Santamaría, R. Menéndez, A. Corma, H. García, Surface area measurement of graphene oxide in aqueous solutions, *Langmuir* 29 (2013) 13443–13448.
- [42] G. Li, L. Wang, H. Ni, C.U. Pittman, Polyhedral oligomeric silsesquioxane (POSS) polymers and copolymers: a review, *J. Inorg. Organomet. Polym.* 11 (2001) 123–154.
- [43] W.-H. Liao, S.-Y. Yang, J.-Y. Wang, H.-W. Tien, S.-T. Hsiao, Y.-S. Wang, S.-M. Li, C.-C.M. Ma, Y.-F. Wu, Effect of Molecular chain length on the mechanical and thermal properties of amine-functionalized graphene oxide/polyimide composite films prepared by in situ polymerization, *ACS Appl. Mater. Interfaces* 5 (2013) 869–877.
- [44] M.D. Haw, Jamming, Two-fluid behavior, and “self-filtration” in concentrated particulate suspensions, *Phys. Rev. Lett.* 92 (2004) 185506.
- [45] Y. Liu, J.R. de Bruyn, Start-up flow of a yield-stress fluid in a vertical pipe, *J. Non-Newton. Fluid Mech.* 257 (2018) 50–58.